Matter Wave Diffraction from an Inclined Transmission Grating: Searching for the Elusive ^{4}He Trimer Efimov State

R. Brühl,[1] A. Kalinin,[1] O. Kornilov,[1] J. P. Toennies,[1] G. C. Hegerfeldt,[2] and M. Stoll[2]
[1]*Max-Planck-Institut für Dynamik und Selbstorganisation, Bunsenstraße 10, 37073 Göttingen, Germany*
[2]*Institut für Theoretische Physik, Universität Göttingen, Friedrich-Hund-Platz 1, 37077 Göttingen, Germany*
(Received 3 December 2004; published 2 August 2005)

The size of the helium trimer is determined by diffracting a beam of ^{4}He clusters from a 100 nm period grating inclined by 21°. Because of the bar thickness the projected slit width is roughly halved to 27 nm, increasing the sensitivity to the trimer size. The peak intensities measured out to the eighth order are evaluated via a few-body scattering theory. The trimer pair distance is found to be $\langle r\rangle = 1.1^{+0.4}_{-0.5}$ nm in agreement with predictions for the ground state. No evidence for a significant amount of Efimov trimers is found. Their concentration is estimated to be under 6%, less than expected.

DOI: 10.1103/PhysRevLett.95.063002 PACS numbers: 36.40.Mr, 03.75.Be, 21.45.+v, 33.15.−e

In 1970 Vitali Efimov found a remarkable unexpected property in the notoriously difficult three-body problem [1]. According to Efimov a weakening of the two-body interaction in a system of three identical bosons can lead to the appearance of an infinite number of bound levels, instead of dissociation as one would expect from classical mechanics. This effect is related to the divergence of the atomic scattering length a with decreasing binding energy E_b between two of the particles [2]. In nuclear physics, despite extensive searches, no example for the Efimov effect has been found up to now [3]. At present the most promising candidate is the ^{4}He trimer [4], although there have been recent attempts to identify Efimov molecules in ultracold collisions of Cs atoms [5].

Because of their very weak binding, the existence of the ^{4}He dimer and trimer could only recently be established experimentally by a new technique involving matter wave diffraction [6]. A beam of clusters formed in a cryogenic free jet expansion is directed at a nanostructured $d = 100$ nm period SiN_x transmission grating. Since the cluster de Broglie wavelength λ is inversely proportional to the cluster mass, first order Bragg diffraction peaks for different masses are observed at different angles $\vartheta \approx \lambda/d$, thereby identifying the clusters uniquely. This technique can also be used to measure the spatial extent of the clusters. From an analysis of the ^{4}He dimer diffraction pattern the slit function of the grating could be determined. After accounting for the van der Waals interaction, the slit width reduction was equal to $\frac{1}{2}\langle r\rangle$ [7,8], from which the mean bond length was found to be $\langle r\rangle = 5.2 \pm 0.4$ nm [7]. This extremely large distance is due to the weak binding energy which was estimated to be only $|E_b| = 1.1^{+0.3}_{-0.2}$ mK [7].

For the helium trimer, theory predicts one Efimov state with a similarly weak binding energy of $|E_e| = 2.3$ mK in addition to the ground state with $|E_g| = 126$ mK with corresponding pair distances (bond lengths) $\langle r\rangle = 7.97$ nm and 0.96 nm, respectively [9]. These two s states are expected to be distinguishable by their sizes. However, experiments similar to those for the dimer did not yield conclusive results which, ultimately, was attributed to an insufficient resolution. The present experiment overcomes this limitation by rotating the grating by an angle Θ_0 around an axis parallel to the slits as seen in Fig. 1. At $\Theta_0 = 21°$, due to the thickness of the bars, the projected slit width is more than halved to $s_\perp = 26.9$ nm, providing a good compromise between the improvement in both the ratio $\langle r\rangle/s_\perp$ and the resolution at the expense of total transmission. The apparatus used is otherwise similar to the one described in detail in Ref. [10]. For the trimer measurements the cryogenic source temperatures T_0 and pressures P_0 were varied between $(T_0, P_0) =$ (6.7 K, 1 bar) and (40 K, 50 bar) to produce optimal trimer mole fractions of up to 7% [11]. The collimated beam with a velocity spread $\Delta v/v \leq 2\%$ has a spatial lateral coherence greater than the exposed 100 grating slits. For both atom and trimer measurements the mass spectrometer

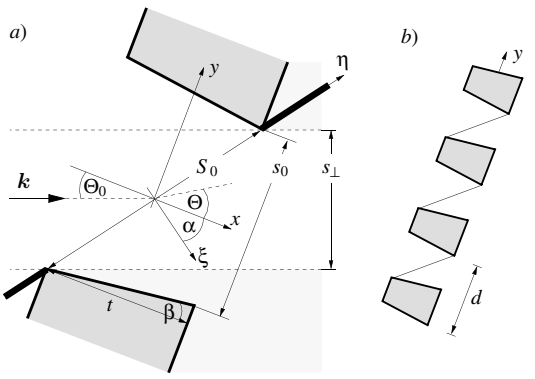

FIG. 1. Diffraction geometry at non-normal incidence: (a) a single slit of width s_0 in a plate of thickness t with a wedge angle β has a projected slit width of $s_\perp$. Both the angle of incidence Θ_0 and the angle Θ are measured relative to the plate normal. The hypothetical thin plate drawn along the η direction with a slit of width $S_0 = \sqrt{(s_0 + t\tan\beta)^2 + t^2}$ at an angle $\alpha = \arcsin(t/S_0)$ relative to the thick plate along the y direction casts the same geometrical shadow as the thick plate. (b) Transmission grating of period d along the y direction.

detector was set at the ^{4}He ion mass. The maximum trimer signal was about 200 counts/secs.

Figure 2(a) shows a diffraction pattern out of a series of altogether 13 taken for various velocities at $\Theta_0 = 18°$ and 21°. The most intense peaks are due to helium atoms. The peak intensities in Fig. 2(b) exhibit an up to 10% deviation from the symmetry ($I_n = I_{-n}$) seen in all previous experiments [12]. This new feature is clearly demonstrated by the contrast $C_n = (I_n - I_{-n})/(I_n + I_{-n})$ displayed in Fig. 2(c). By modifying the theory of Ref. [13] the new measurements could be evaluated to obtain the bond length of the helium trimer $\langle r \rangle = 1.1^{+0.4}_{-0.5}$ nm. Assuming the theoretical values of $\langle r \rangle$ the concentration of Efimov trimers in the beam is estimated to be less than 6%. Since this is significantly smaller than the expected concentration of 10% the existence of an Efimov state in $^4He_3$ must be questioned.

From atom beam transmission experiments [10] the grating bars are found to have a thickness $t = 118.3 \pm 0.5$ nm and their inner faces have a wedge angle $\beta = 6.7 \pm 0.5°$ with the direction perpendicular to the grating (Fig. 1). Since the angle of inclination (angle of incidence) Θ_0 exceeds the wedge angle β the upper bar faces (Fig. 1) are shadowed by the front edges of the bars. Obviously in this geometry the opening (s_0 in Fig. 1) used for calculating the scattering amplitude at normal incidence [7,8] is no longer appropriate. Instead the slit is modeled by a diagonal opening of width S_0 in a thin plate along the η axis (Fig. 1) which casts the same geometrical shadow as the original slit [14]. Complications from scattering from the upper bar faces are not expected since the cluster de

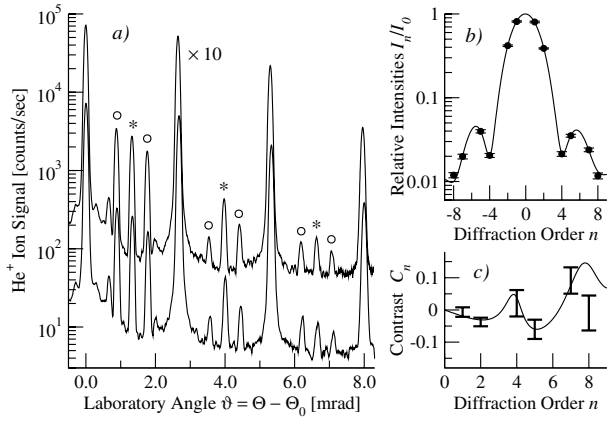

FIG. 2. (a) ^{4}He diffraction pattern at $\Theta_0 = 21°$ angle of incidence measured for the source conditions $(T_0, P_0) = (16.5\ \mathrm{K}, 7.0\ \mathrm{bar})$ corresponding to a trimer de Broglie wavelength of $\lambda = 0.83$ Å. The signal at negative diffraction angles has been shifted upwards by a factor 10 and mirrored onto the positive side for comparison. The trimer diffraction peaks are marked by circles, dimer peaks by stars. (b) Relative trimer peak intensities I_n/I_0. (c) Corresponding contrast $C_n = (I_n - I_{-n})/(I_n + I_{-n})$. The curves in (b) and (c) are best-fit calculations based on Eq. (6).

Broglie wavelength $\lambda \approx 1$ Å is much smaller than the slit width such that the diffraction is concentrated in a small range of angles of the order of $\vartheta = \Theta - \Theta_0 \simeq \lambda/s_\perp \approx 2°$, much smaller than $\Theta_0 - \beta \approx 14°$. Modeling the incident beam by a plane wave of wave vector $\boldsymbol{k}$ with $k = |\boldsymbol{k}| = 2\pi/\lambda$ and imposing Kirchhoff boundary conditions along the slit S_0 leads to the following expression for the scattering amplitude of the diagonal slit [8,15]

$$f_{\mathrm{slit}}(\Theta) = \frac{\cos(\Theta_0 + \alpha)}{\sqrt{\lambda}} \int_{-S_0/2}^{S_0/2} d\eta e^{-iK(\Theta)\eta} \tau(\eta), \qquad (1)$$

where the bar thickness enters through $\sin\alpha = t/S_0$ and

$$K(\Theta) = k[\sin(\Theta + \alpha) - \sin(\Theta_0 + \alpha)] \qquad (2)$$

is the wave vector transfer along the slit direction (η axis). The transmission function $\tau(\eta)$ in Eq. (1) accounts for the size of the cluster [7] as well as the van der Waals potential $-C_3/l^3$ between the atoms and the bar material [8], where l is the distance from the surface.

The inclined transmission grating consists of many slits aligned along the y axis with period d [Fig. 1(b)]. The periodicity then gives rise to sharp principal diffraction maxima located at the Bragg angles Θ_n satisfying

$$k[\sin\Theta_n - \sin\Theta_0] = 2\pi n/d \qquad (3)$$

for $n = 0, \pm 1, \pm 2$, etc. [16]. Solving Eq. (3) for Θ_n and inserting into Eq. (2) yields $K(\Theta_n)$ at which the scattering amplitude determining the intensity of the nth diffraction order is to be evaluated. By expanding through second order in n, $K(\Theta_n)$ can be expressed as

$$\frac{K(\Theta_n)}{\cos(\Theta_0 + \alpha)} \approx \frac{2\pi n}{d\cos\Theta_0} + \lambda \frac{\tan\Theta_0 - \tan(\Theta_0 + \alpha)}{4\pi} \times \left(\frac{2\pi n}{d\cos\Theta_0}\right)^2.$$

Thus, although the scattering amplitude itself is even under the change of the sign of $K(\Theta)$, it is probed at a wave vector transfer for which $K(\Theta_n) \neq -K(\Theta_{-n})$. The origin of the experimentally observed asymmetry $I_n \neq I_{-n}$ of the diffraction pattern lies, therefore, in the nonalignment of the slits S_0 (η axis) and the direction of periodicity (y axis). The asymmetry decreases with λ because for a smaller de Broglie wavelength less clusters are diffracted into the regions shaded by the slits (Fig. 1). Clearly, for $\alpha = 0$ (thin grating) the symmetric case is recovered. Supplementary calculations indicate that the van der Waals surface interaction has only a minor effect on the asymmetry.

Introducing the functions $\Phi^+(K)$ and $\Phi^-(K)$ [8]

$$\Phi^{\pm}(K) = \int_0^{S_0/2} d\eta e^{\pm iK\eta} \frac{\frac{\partial}{\partial\eta}\tau[\pm(S_0/2 - \eta)]}{\tau(0)} \qquad (4)$$

allows the scattering amplitude to be expressed as

$$f_{\rm slit}(\Theta) = \frac{\cos(\Theta+\alpha)}{\sqrt{\lambda}}\tau(0) \times \frac{e^{iK(\Theta)S_0/2}\Phi^-(K(\Theta)) - e^{-iK(\Theta)S_0/2}\Phi^+(K(\Theta))}{iK(\Theta)}. \quad (5)$$

To conveniently combine the functions $\Phi^{\pm}(K)$ with the exponentials in Eq. (5) their logarithms are expanded in a power series: $\ln\Phi^{\pm}(K) = \Sigma_{j=1}^{\infty}(\pm iK)^j R_j^{\pm}/j!$, which uniquely defines the complex numbers $R_j^{\pm}$ known as the cumulants. For example, the first cumulants are given by $R_1^{\pm} = \pm\int_0^{\pm S_0/2} d\eta[1-\tau(\eta)]$ and account for the different transmission in the two halves of the slit. For diffraction orders $|n| \lesssim 8$ encountered experimentally it is sufficient to retain only the first two terms of this expansion. Inserting them into Eq. (5) the nth order diffraction intensity becomes, to good approximation,

$$\frac{I_n}{I_0} = \frac{e^{-K(\Theta_n)^2\Sigma^2}e^{-K(\Theta_n)\Gamma}}{(\frac{K(\Theta_n)\sqrt{S_{\rm eff}^2+\Delta^2}}{2})^2}\left[\sin^2\left(\frac{K(\Theta_n)S_{\rm eff}}{2}\right) + \sinh^2\left(\frac{K(\Theta_n)\Delta}{2}\right)\right]. \quad (6)$$

Here, the effective slit width $S_{\rm eff} = S_0 - {\rm Re}\,(R_1^+ + R_1^-)$ accounts for the reduction of the geometrical slit width S_0 due to the surface interaction as well as the finite cluster size. The exponential involving $\Sigma = \sqrt{{\rm Re}\,(R_2^+ + R_2^-)/2} \approx 5$ nm includes the Debye-Waller attenuation due to slit width irregularities and also accounts for cluster breakup [7,8]. The surface interaction removes the intensity zeros through the term involving $\Delta = {\rm Im}\,(R_1^+ + R_1^-) \approx 10$ nm and contributes weakly to the asymmetry through $\Gamma = {\rm Im}\,(R_1^+ - R_1^-) \approx 1.5$ nm.

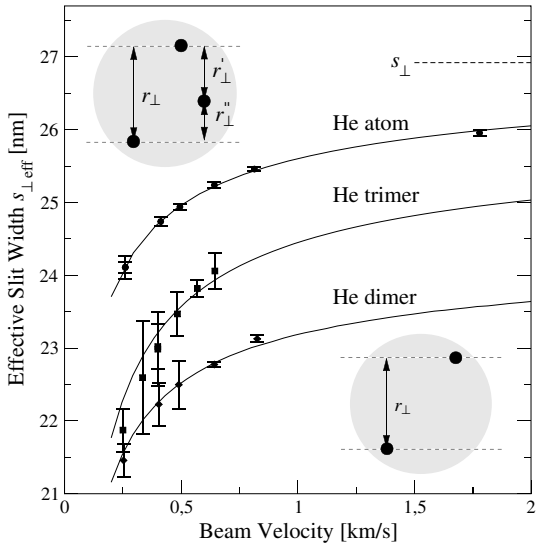

FIG. 3. Projected effective slit widths $s_{\perp\rm eff} = S_{\rm eff}\cos(\Theta_0+\alpha)$ measured at different beam velocities at an angle of incidence $\Theta_0 = 21°$ for ^{4}He, ^{4}He$_2$, and ^{4}He$_3$. The curves represent best fits of Eq. (7) for ^{4}He$_3$ and analogous expressions for ^{4}He and ^{4}He$_2$. Their high velocity limits are given by $s_\perp$ for ^{4}He, by $s_\perp - \frac{1}{2}\langle r\rangle$ for ^{4}He$_2$, and by $s_\perp - \frac{3}{4}\langle r\rangle$ for ^{4}He$_3$. The insets illustrate the ''widths'' traced out by the clusters along their flight paths (see text).

Experimental values for $S_{\rm eff}$ were obtained from fits of the intensity formula Eq. (6) to trimer diffraction patterns [Fig. 2(b)] measured for $T_0 = 6.7$–40 K. In Fig. 3 the projected effective slit widths $s_{\perp\rm eff} = S_{\rm eff}\cos(\Theta_0+\alpha)$ for ^{4}He, ^{4}He$_2$, and ^{4}He$_3$ at $\Theta_0 = 21°$ are plotted as functions of the beam velocity. The atom data were used to determine the projected slit width $s_\perp = 26.92 \pm 0.02$ nm [8] and $C_3 = 0.113 \pm 0.02$ meV nm^3 was taken from Ref. [8]. From Fig. 3 the slit width reduction at a velocity of 0.64 km/s is about 1.2 nm for trimers and 2.5 nm for dimers. Moreover, the dimer curve runs almost parallel to the atom curve, suggesting that, due to the large extent of the dimer wave function, on average only one of its atoms interacts with the surface. In contrast, the steeper slope of the trimer curve indicates the contribution of more than one atom, also confirming the relative compactness of this cluster.

The quantum mechanical few-body scattering approach of Ref. [13] can be extended from dimers to trimers. The size effect is caused by the width of the trimer perpendicular to its incident direction. This width can be expressed by $\langle|r_\perp| + |r'_\perp| + |r''_\perp|\rangle/2$ where the three distances are defined in the upper inset of Fig. 3. For the homonuclear ^{4}He$_3$ this quantity reduces to $3\langle|r_\perp|\rangle/2$. Moreover, since the pair interactions are dominated by the shallow s-wave dimer state, the homogeneous Faddeev equations [17] can be used to express the width in terms of the trimer bond length as $3\langle r\rangle/4$. The complete expression for $s_{\perp\rm eff}$, which includes the surface interaction, is then found to be

$$s_{\perp\rm eff} = s_\perp - \frac{3}{4}\langle r\rangle - \zeta\,{\rm Re}\left\{\int_0^{S_0/2} \times d\eta\left[1-\tau_{\rm at}(\eta)\tau_{\rm at}\left(\eta-\frac{1}{2}\frac{\langle r\rangle}{\zeta}\right)\tau_{\rm at}\left(\eta-\frac{5}{8}\frac{\langle r\rangle}{\zeta}\right)\right] + \int_{-S_0/2}^{0} d\eta\left[1-\tau_{\rm at}(\eta)\tau_{\rm at}\left(\eta+\frac{1}{2}\frac{\langle r\rangle}{\zeta}\right) \times \tau_{\rm at}\left(\eta+\frac{5}{8}\frac{\langle r\rangle}{\zeta}\right)\right]\right\}, \quad (7)$$

where $\zeta = \cos(\Theta_0+\alpha)$ was used. The term in curly braces in Eq. (7) accounts for the surface interaction via the atom transmission functions $\tau_{\rm at}(\eta)$ [8]. As seen in Fig. 3 this term varies between 2–3 nm in the experimental range of 0.25–0.64 km/s.

Using Eq. (7) the best-fit curve for the trimer based on seven diffraction patterns taken at $\Theta_0 = 21°$ was obtained for the bond length $\langle r\rangle = 1.0^{+0.5}_{-0.7}$ nm. A second series of six diffraction patterns taken at $\Theta_0 = 18°$ yielded

$\langle r\rangle = 1.2^{+0.5}_{-0.8}$ nm which confirms, within the error bars, the reproducibility. The average of both results, $\langle r\rangle = 1.1^{+0.4}_{-0.5}$ nm, agrees well with the theoretical prediction of 0.96 nm [9] for the $^4He_3$ ground state. With the theoretical values for $\langle r\rangle$ a simulation of the diffraction pattern for various concentrations indicates that the upper experimental limit is consistent with less than 6% Efimov trimers, reducing substantially the previous value of 15% [18].

At present it is not possible to predict rigorously the concentration of Efimov molecules in free jet expansions. In a recent study [19] it was discovered, however, that the mole fractions of small helium clusters can be described with remarkable accuracy by a simple sudden freeze model mentioned in Ref. [11]. From the measured trimer mole fraction of 5.5% (Fig. 2) the trimer sudden freeze temperature is calculated using Eq. (41) of Ref. [11] to be $T_\infty = 57$ mK. Assuming equilibrium, then, the fraction of trimers in the Efimov state, given by $[1 + \exp(-E_g/kT_\infty)]^{-1}$, is equal to 10% at this temperature. In the previous analysis of the mole fractions [11,20] the largest correction accounted for the attenuation due to collisions with the residual He gas in the source chamber. In order to investigate this effect previous studies of ground state trimers in collisions with Kr atoms [18] were extended to He atom targets. The results indicate that the trimer ground state has only a 7% smaller cross section than that predicted for the Efimov trimer of 3 times the atom-atom cross section [18]. Thus we can rule out any significant difference between collisional attenuation of the ground state and Efimov trimers so that the fraction of 10% will not be affected.

We feel that the difference between the expectation of 10% and the experimental upper limit of 6% is sufficient to entertain the possibility that the $^4He_3$ Efimov state does, in fact, not exist despite the over 40 theory publications which have appeared since 1977. Since all calculations have been carried out for adiabatic two-body potentials, which have been tested both experimentally [7] and by numerical methods [21], it is still conceivable that the presence of the Efimov state is affected by the sum of so far neglected small corrections to the potentials, such as a three-body contribution to the interaction [22], retardation, or nonadiabatic effects [23]. For example, Gdanitz [23] showed that the latter can modify the scattering length by about 5%–10%. However, a solution of the Faddeev equations based on a separable potential reveals that such a modification alone cannot render the Efimov state unbound.

In future experiments a promising approach to detect Efimov $^4He_3$ could involve sampling the sizes of clusters effusing from a Knudsen cell, thereby ruling out collisional deexcitation. Then the Efimov and ground state molecules would have small but nearly equal concentrations. To compensate for the loss in signal the trimer mole fraction could be increased by going to a much higher P_0 while reducing the orifice diameter. A new, much more sensitive detector currently under development may make such experiments possible.

We are indebted to T. Savas for providing the transmission grating and thank T. Köhler for stimulating discussions.

[1] V. Efimov, Phys. Lett. **33B**, 563 (1970).
[2] J. Lekner, Mol. Phys. **23**, 619 (1972).
[3] A. S. Jensen, K. Riisager, D. V. Fedorov, and E. Garrido, Rev. Mod. Phys. **76**, 215 (2004).
[4] T. K. Lim, S. K. Duffy, and W. C. Damert, Phys. Rev. Lett. **38**, 341 (1977).
[5] C. Chin, V. Vuletic, A. J. Kerman, and S. Chu, Nucl. Phys. **A684**, 641c (2001).
[6] W. Schöllkopf and J. P. Toennies, Science **266**, 1345 (1994).
[7] R. E. Grisenti, W. Schöllkopf, J. P. Toennies, G. C. Hegerfeldt, T. Köhler, and M. Stoll, Phys. Rev. Lett. **85**, 2284 (2000).
[8] R. E. Grisenti, W. Schöllkopf, J. P. Toennies, G. C. Hegerfeldt, and T. Köhler, Phys. Rev. Lett. **83**, 1755 (1999).
[9] P. Barletta and A. Kievsky, Phys. Rev. A **64**, 042514 (2001); A. K. Motovilov, W. Sandhas, S. A. Sofianos, and E. A. Kolganova, Eur. Phys. J. D **13**, 33 (2001); E. Braaten and H.-W. Hammer, Phys. Rev. A **67**, 042706 (2003).
[10] R. E. Grisenti, W. Schöllkopf, J. P. Toennies, J. R. Manson, T. A. Savas, and H. I. Smith, Phys. Rev. A **61**, 033608 (2000).
[11] L. W. Bruch, W. Schöllkopf, and J. P. Toennies, J. Chem. Phys. **117**, 1544 (2002).
[12] As seen in Fig. 2 the diffraction angles $\vartheta_n = \Theta_n - \Theta_0$ are also asymmetric ($\vartheta_n \neq -\vartheta_{-n}$) in agreement with the Bragg law Eq. (3). However, this effect is unrelated to the intensity asymmetry.
[13] G. C. Hegerfeldt and T. Köhler, Phys. Rev. A **57**, 2021 (1998); **61**, 23606 (2000).
[14] This argument can also be derived formally from diffraction theory under the condition $\lambda \ll t, S_0$. See, e.g., P. M. Morse and H. Feshbach, *Methods of Theoretical Physics* (McGraw-Hill, New York, 1953), Sect. 11.4, p. 1551.
[15] M. Born and E. Wolf, *Principles of Optics* (Pergamon, New York, 1959), Sect. 11.3.
[16] For $n2\pi/(kd) \ll 1$ one has $\vartheta_n = \Theta_n - \Theta_0 \approx n2\pi/(kd\cos\Theta_0)$, as used in Ref. [10].
[17] A. G. Sitenko, *Lectures in Scattering Theory* (Pergamon, New York, 1971).
[18] A. Kalinin, O. Kornilov, L. Rusin, J. P. Toennies, and G. Vladimirov, Phys. Rev. Lett. **93**, 163402 (2004).
[19] A. Kalinin, O. Kornilov, W. Schöllkopf, and J. P. Toennies, Phys. Rev. Lett. (to be published).
[20] R. Kariotis, O. Kornilov, and L. W. Bruch, J. Chem. Phys. **121**, 3044 (2004).
[21] J. B. Anderson, J. Chem. Phys. **120**, 9886 (2004).
[22] I. Røeggen and J. Almlöf, J. Chem. Phys. **102**, 7095 (1995).
[23] R. J. Gdanitz, Mol. Phys. **99**, 923 (2001).